

International Journal of Bifurcation and Chaos, Vol. 33, No. 15 (2023) 2350180 (22 pages) © World Scientific Publishing Company

DOI: 10.1142/S0218127423501808

Bifurcation Analysis of a New Aquatic Ecological Model with Aggregation Effect and Harvesting

Chenyu Liang

Department of Mathematics, Hangzhou Normal University, Hangzhou 311121, P. R. China

Department of Mathematics, China Jiliang University, Hangzhou 310018, P. R. China

Hangjun Zhang*

School of Engineering, Hangzhou Normal University, Hangzhou 311121, P. R. China zhanghangjun@hznu.edu.cn

Yancong Xu*

Department of Mathematics, China Jiliang University, Hangzhou 310018, P. R. China Yancongx@cjlu.edu.cn

Libin Rong

Department of Mathematics, University of Florida, Gainesville 32611, USA

Received June 16, 2023; Revised September 7, 2023

In this paper, we investigated the dynamics of the interaction between Microcystis aeruginosa and filter-feeding fish in a new aquatic ecological model and considered the effects of aggregation and harvesting and focused on studying the critical threshold conditions through the analysis of saddle-node bifurcation, Hopf bifurcation, and Bogdanov–Takens bifurcation. We also conducted numerical simulations to illustrate our findings and provided biological interpretations. The results obtained indicate that the aggregation effect or harvesting can disrupt the coexistence of Microcystis aeruginosa and filter-feeding fish. The filter-feeding fish population may go extinct while the Microcystis aeruginosa population could survive. We identified the importance of finding an appropriate timing for harvesting Microcystis aeruginosa in order to promote the growth of the filter-feeding fish population. This optimal timing may be influenced by the carrying capacity of Microcystis aeruginosa. Taken together, our study sheds light on the dynamics of Microcystis aeruginosa and filter-feeding fish in an aquatic ecosystem, highlighting the critical role of aggregation, harvesting, and timing in determining the coexistence and survival of these species.

Keywords: Aquatic ecological model; Microcystis aeruginosa; filter feeding fish; Hopf bifurcation; Bogdanov-Takens bifurcation.

^{*}Authors for correspondence

1. Introduction

In recent years, the severity of algal blooms has increased due to factors such as global warming, elevated atmospheric carbon dioxide levels, water eutrophication, and other environmental changes. Algal blooms have emerged as a significant global environmental concern. Biological control has been proved to be the most effective method for suppressing algal blooms. This approach leverages the ecological relationships of predation among different organisms in the ecosystem, specifically using filter-feeding fish to filter and consume algae, thereby improving the structure of algal populations and reducing bloom concentrations. Introducing filter-feeding fish is an economical, efficient, and rational solution.

One of the primary causes of algal blooms is the aggregation and migration of algal populations within water bodies. In natural lakes and rivers, Microcystis often exists in aggregated forms. There are two primary mechanisms for colony formation: aggregation of individual cells into gel colonies and the division and colonization of single cells, with the resulting daughter cells effectively aggregating to form a population. In complex water environments, these two aggregation modes coexist. Consequently, Microcystis continuously accumulates, undergoes vertical migration, rises to the lake surface to form algal aggregates, and experiences repeated accumulation and migration under the influence of converging or diverging lake currents, eventually resulting in algal blooms. Therefore, studying the dynamic behavior of Microcystis is essential.

After extensive literature review, we observed a relative scarcity of research on mathematical models concerning the aggregation of algae in aquatic ecosystems. Some researchers have explored the influence of algal aggregation on algal blooms and the impact of filter-feeding fish on algae from the perspectives of aquatic ecology and population science Huang et al., 2023; Xie & Liu, 2001; Zhang et al., 2011; Zhou et al., 2013; Duan et al., 2019; Chen & Lurling, 2020; Zhang et al., 2023; Duan et al., 2020; Pal et al., 2020; Tang et al., 2017; Kolmakov, 2014. Huang et al. 2023 conducted a study on the effects of various growth conditions, such as water temperature, pH value, light, and nutrients, on the formation of trihalomethanes (THMFPs) in four components of Microcystis aeruginosa: hydrophilic extracellular organic matter (HPI-EOM), hydrophobic EOM (HPO-EOM),

hydrophilic intracellular organic matter (HPI-IOM), and hydrophobic IOM (HPO-IOM). Their findings revealed that THMFP in EOM is sensitive to growth conditions and independent of algal density. Chen and Lurling [2020] investigated the rapid aggregation and colony formation of Microcystis caused by calcium ions through cell adhesion. Higher concentrations of calcium ions did not impact the microcystin content but promoted the binding of extracellular polysaccharides, leading to the formation of larger colonies and increased Microcystis accumulation on surfaces. Zhang et al. [2023] studied the bioaccumulation and detoxification of microcystin-LR (MC-LR). Duan et al. [2020] explored the effects of exposure to Microcystis aeruginosa (MA) and its produced microcystins (MC-LR) on gut microbiota variation and immune response in Litopenaeus vannamei. The results demonstrated significant histological changes and apoptosis characteristics due to MA and MC-LR exposure, leading to alterations in histopathology and gut microbiota, including Lactobacillus albus, as well as increased oxidative stress in the shrimp gut. These studies provide valuable insights into the dynamics and effects of algal aggregation and its interactions with environmental factors, toxins, and organisms in aquatic ecosystems. However, further research is needed to enhance our understanding of this complex phenomenon.

Harvesting practices are commonly employed in predator-prey systems, and bifurcation methods have been utilized in various studies to analyze these systems Lu et al., 2022; Yang et al., 2023; Liu & Zhang, 2016; Auger *et al.*, 2006; Sen et al., 2022; Cui & Song, 2004; Ly et al., 2013a; Xu et al., 2020; Ly et al., 2013b; Rihan et al., 2020; Zhu et al., 2023; Yu et al., 2014. Ly et al. 2019 proposed and investigated a predator-prey model with selective nonlinear harvesting for both the prey and predator. They developed a Holling II functional response prey-predator model with harvesting in a two-patch environment: a free fishing zone (patch 1) and a reserve zone (patch 2) where fishing is strictly prohibited. They also explored two types of predator-prey models incorporating nonsmooth and noncontinuous harvesting. Liu et al. [2021] constructed an aquatic amensalism model with nonselective harvesting and an Allee effect to study the inhibitory mechanism of algicidal bacteria on algae. Li et al. 2021 and Huang et al. 2022 investigated a new aquatic ecological model that incorporates

the aggregation effect and Allee effect to describe the complex dynamics of Microcystis aeruginosa. In summary, significant progress has been made in the field of ecological mathematical models and population dynamics. However, the development of aquatic ecological models, particularly those incorporating the effects of algae aggregation and harvesting, has been relatively slow. Further research is needed to advance our understanding in this area.

Li et al. [2021] and Huang et al. [2022] considered the following aquatic ecological model with aggregation effect

$$\dot{N} = Nr \left(1 - \frac{N}{K_1} \right) - \frac{\alpha_1 P(N - m_1)}{c_1 - m_1 + N},
\dot{P} = \frac{\alpha_1 \beta_1 P(N - m_1)}{c_1 - m_1 + N} + d_1 P \left(1 - \frac{N}{K_1} \right) - \gamma_1 P,$$
(1)

where N and P represent the density of Microcystis aeruginosa and filter-feeding fish at time T, respectively. $Nr(1-\frac{N}{K_1})$ denotes the growth kinetics function of Microcystis aeruginosa with intrinsic growth rate r and maximum environmental capacity K_1 . The function $\frac{\alpha_1 P(N-m_1)}{c_1-m_1+N}$ describes the aquatic ecological mechanism with grazing coefficient α_1 , half-saturation constant c_1 and Microcystis aeruginosa aggregation parameter m_1 . The function $d_1P(1-\frac{N}{K_1})$ describes how Microcystis aeruginosa affects the abundance of filter-feeding fish with an intrinsic growth rate d_1 , and $\frac{\alpha_1\beta_1P(N-m_1)}{c_1-m_1+N}$ describes how Microcystis aeruginosa aggregation affects the abundance of filter-feeding fish population with the absorption coefficient β_1 . The filter-feeding fish population P is subject to a death function $\gamma_1 P$ with a mortality coefficient γ_1 . This function takes into account the aggregation of Microcystis aeruginosa and captures the dynamic relationship between Microcystis aeruginosa and filter-feeding fish. Since Microcystis aeruginosa consists of numerous cells, the model considers the impact of both algal aggregation and algal monomers on filter-feeding fish. In [Lv et al., 2019], the authors utilized a harvesting functional form $\frac{hN}{h+N}$, which represents the harvesting of Microcystis aeruginosa. This harvesting process is employed to prevent algal blooms as Microcystis aeruginosa can produce microcystins (MCs) that are highly hepatotoxic during their growth and decomposition. These MCs can cause fish poisoning and death. Therefore, when algae grow rapidly, artificial harvesting is performed in lakes to control the algal population.

Motivated by Li et al., 2021 and Huang et al., 2022, we consider the following aquatic ecological model with aggregation effect and harvesting

$$\dot{N} = Nr \left(1 - \frac{N}{K_1} \right) - \frac{\alpha_1 P(N - m_1)}{c_1 - m_1 + N} - \frac{hN}{h + N},$$

$$\dot{P} = \frac{\alpha_1 \beta_1 P(N - m_1)}{c_1 - m_1 + N} + d_1 P \left(1 - \frac{N}{K_1} \right) - \gamma_1 P,$$
(2)

where $\frac{hN}{h+N}$ is the harvesting function with the maximum harvesting rate of Microcystis aeruginosa h. In the subsequent analysis, our focus will be on examining the dynamics of an aquatic ecological model that incorporates the aggregation effect and harvesting. This analysis will involve studying the equilibrium points and conducting bifurcation analysis to elucidate the transition and interaction mechanisms between Microcystis aeruginosa and filter-feeding fish.

The remaining sections of the paper are organized as follows. In Sec. 2 we examine the existence and stability of equilibria in the model. In Sec. 3 we provide a comprehensive bifurcation analysis, including the investigation of saddle-node bifurcation, Bogdanov—Takens bifurcation, and Hopf bifurcation. Section 4 presents numerical simulation analysis and showcases phase portraits. Finally, the paper concludes with a summary of findings and a discussion of the results.

2. Existence and Stability of Equilibria

We rescale model (2) by

$$N = c_1 x$$
, $P = hy$, $T = \frac{t}{x}$.

Model (2) becomes

$$\frac{dx}{dt} = x\left(1 - \frac{x}{k}\right) - \frac{py(x-m)}{1+x-m} - \frac{qx}{x+1},$$

$$\frac{dy}{dt} = \frac{ay(x-m)}{1+x-m} + by\left(1 - \frac{x}{k}\right) - cy,$$
(3)

where

$$a = \frac{\alpha_1 \beta_1}{r}, \quad b = \frac{d_1}{r}, \quad c = \frac{\gamma_1}{r}, \quad p = \frac{\alpha_1 h}{c_1 r},$$

$$q = \frac{h}{r c_1}, \quad m = \frac{m_1}{c_1}, \quad k = \frac{K_1}{c_1}$$

and a, b, c, p, q, m, k are all positive parameters.

From model (B), we consider the Microcystis aeruginosa isocline vertically and the filter-feeding fish isocline horizontally, and obtain

$$y = \frac{x(1+x-m)(x^2+(1-k)x+k(q-1))}{kp(x+1)(m-x)},$$

$$\frac{a(x-m)}{1+x-m} + b\left(1 - \frac{x}{k}\right) - c = 0 \quad \text{or} \quad y = 0.$$
(4)

Considering the biological significance and the characteristics of isoclines, we can conclude that the existence of an internal equilibrium is conditional, and it requires the conditions m < x < k and $x^2 + (1-k)x + k(q-1) < 0$ to be satisfied. We find that model (2) has an equilibrium $E_0(0,0)$ if $m \neq 1$ and

two boundary equilibria $E_{01}(\frac{k-1+\sqrt{(k+1)^2-4kq}}{2},0)$, $E_{02}(\frac{k-1-\sqrt{(k+1)^2-4kq}}{2},0)$ when $(k+1)^2 \geq 4kq$. To find the positive equilibria of model (2), we set

$$\frac{a(x-m)}{x+1-m} + b\left(1 - \frac{x}{k}\right) - c = 0,\tag{5}$$

which yields

$$bx^{2} + (b - bm + ck - ak - bk)x$$
$$+ k(am + bm - cm + c - b) = 0.$$
 (6)

From (5) and (6), model (2) has at most two positive equilibria $E_1(x_1, y_1)$ and $E_2(x_2, y_2)$, which may merge into a unique positive equilibrium $E_*(x_*, y_*)$, where

$$x_{1} = \frac{ak + bk - ck + bm - b - \sqrt{(b - bm + ck - ak - bk)^{2} - 4bk(am + bm - cm + c - b)}}{2b},$$

$$x_{2} = \frac{ak + bk - ck + bm - b + \sqrt{(b - bm + ck - ak - bk)^{2} - 4bk(am + bm - cm + c - b)}}{2b},$$

$$x_{*} = \frac{ak + bk - ck + bm - b}{2b}.$$
(7)

The discriminant of (6) is

$$\Delta = (b - bm + ck - ak - bk)^{2}$$
$$-4bk(am + bm - cm + c - b)$$
(8)

and we have

$$x_{1} + x_{2} = \frac{ak + bk - ck + bm - b}{b},$$

$$x_{1}x_{2} = \frac{k(am + bm - cm + c - b)}{b}.$$
(9)

Note that $\Delta \geq 0$ is equivalent to

$$\frac{ak + bk - ck + b - 2\sqrt{abk}}{b}$$

$$\leq m \leq \frac{ak + bk - ck + b + 2\sqrt{abk}}{b}.$$

Let

$$m_1 = \frac{ak + bk - ck + b - 2\sqrt{abk}}{b},$$

$$m_2 = \frac{ak + bk - ck + b + 2\sqrt{abk}}{b},$$

$$m_* = \frac{(ak + bk - ck + b \pm 2\sqrt{abk})}{b},$$

$$(10)$$

then we have the following existence conditions of equilibria in model (2).

Theorem 1. System (2) may have two boundary equilibria $E_{01,02}(\frac{-1+k\pm\sqrt{(k+1)^2-4kq}}{2},0)$ if $(k+1)^2-4kq \ge 0$ and the origin $E_0(0,0)$ exists when $m \ne 1$. Moreover,

- (1) When $m_1 \le m \le m_2$ (i.e. $\Delta > 0$),
 - (a) If (a+b-c)m+c-b < 0 and k[(a+b-c)m+2c-2b-a] > bm-2b, system (2) has a unique positive equilibrium;
 - (b) If $0 < \frac{k(a+b-c)+b(m-1)}{2b} < 1$, k[(a+b-c)m+2c-2b-a] > bm-2b and am+bm-cm+c-b > 0, system (2) has two positive equilibria.
- (2) System (2) has a unique positive equilibrium if and only if $m = m_*$ (i.e. $\Delta = 0$) and 0 < k(a+b-c) + b(m-1) < 2b.
- (3) System (2) has no positive equilibrium in other conditions. Here m_1 , m_2 and m_* are defined by (10).

Now, we will analyze the local stability of the equilibria of model (2). We start by examining the

origin $E_0(0,0)$ when $m \neq 1$. The Jacobian matrix of model (2) at $E_0(0,0)$ is

$$J(E_0) = \begin{bmatrix} 1 - q & \frac{mp}{1 - m} \\ 0 & -\frac{am}{1 - m} + b - c \end{bmatrix}, \quad (11)$$

which has two eigenvalues

$$\lambda_1 = 1 - q, \quad \lambda_2 = -\frac{am}{1 - m} + b - c.$$

We obtain the following results.

Theorem 2. Under the condition $m \neq 1$,

- $\begin{array}{l} (1) \ \ When \ 1-q<0, \ -\frac{am}{1-m}+b-c>0 \ \ or \ 1-q>0, \\ -\frac{am}{1-m}+b-c<0, \ E_0(0,0) \ \ is \ a \ saddle. \end{array}$
- (2) When 1 q < 0, $-\frac{am}{1-m} + b c < 0$,
- (a) $E_0(0,0)$ is a stable node as q $\frac{(c-a-b)m+b-c+m-1}{m-1};$
- (b) $E_0(0,0)$ is a sink as $q = \frac{(c-a-b)m+b-c+m-1}{m-1}$
- (3) When 1 q > 0, $-\frac{am}{1-m} + b c > 0$,
- (a) $E_0(0,0)$ is an unstable node as $q \neq \frac{(c-a-b)m+b-c+m-1}{m-1}$;
- (b) $E_0(0,0)$ is a source as $q = \frac{(c-a-b)m+b-c+m-1}{m-1}$

Next, we study the type of another two boundary equilibria $E_{01,02}(\frac{k-1\pm\sqrt{(k+1)^2-4kq}}{2},0)$ when $(k+1)^2-4kq\geq 0$. The Jacobian matrices of model (2) at $E_{01.02}$ are, respectively,

$$J(E_{01}) = \begin{bmatrix} \lambda_3 & -\frac{p(\sqrt{(k+1)^2 - 4kq} - k + 2m + 1)}{\sqrt{(k+1)^2 - 4kq} - k + 2m - 1} \\ 0 & \lambda_4 \end{bmatrix}$$
(3) If $\lambda_3 < 0$, $\lambda_4 < 0$, $E_{01}(\frac{-1 + k - \sqrt{(k+1)^2 - 4kq}}{2}, 0)$ is a stable focus or node;
$$(4) \text{ If } \lambda_5 \lambda_6 < 0, E_{02}(\frac{-1 + k + \sqrt{(k+1)^2 - 4kq}}{2}, 0) \text{ is a stable};$$

and

$$J(E_{02}) = \begin{bmatrix} \lambda_5 & -\frac{p(\sqrt{(k+1)^2 - 4kq} + k - 2m - 1)}{\sqrt{(k+1)^2 - 4kq} + k - 2m + 1} \\ 0 & \lambda_6 \end{bmatrix},$$

where

$$\lambda_{3} = \frac{\sqrt{(k+1)^{2} - 4kq} + 1}{k}$$

$$-\frac{4q}{(-\sqrt{(k+1)^{2} - 4kq} + k + 1)^{2}},$$

$$\lambda_{4} = \frac{a(\sqrt{(k+1)^{2} - 4kq} - k + 2m + 1)}{\sqrt{(k+1)^{2} - 4kq} - k + 2m - 1}$$

$$+\frac{b(\sqrt{(k+1)^{2} - 4kq} + k + 1)}{2k} - c,$$

$$\lambda_{5} = \frac{1 - \sqrt{(k+1)^{2} - 4kq}}{k}$$

$$-\frac{4q}{(\sqrt{(k+1)^{2} - 4kq} + k + 1)^{2}},$$

$$\lambda_{6} = \frac{a(\sqrt{(k+1)^{2} - 4kq} + k - 2m - 1)}{\sqrt{(k+1)^{2} - 4kq} + k - 2m + 1}$$

$$+\frac{b(-\sqrt{(k+1)^{2} - 4kq} + k + 1)}{2k} - c.$$

Then the eigenvalues of the Jacobian matrix (12) are λ_3, λ_4 and the eigenvalues of the Jacobian matrix (13) are λ_5, λ_6 . We can obtain the following results.

Theorem 3. When $(k+1)^2 - 4kq > 0$.

- (1) If $\lambda_3 \lambda_4 < 0$, $E_{01}(\frac{-1+k-\sqrt{(k+1)^2-4kq}}{2},0)$ is a
- (2) If $\lambda_3 > 0$, $\lambda_4 > 0$, $E_{01}(\frac{-1+k-\sqrt{(k+1)^2-4kq}}{2}, 0)$ is an unstable focus or node;

- (5) If $\lambda_5 > 0$, $\lambda_6 > 0$, $E_{02}(\frac{-1+k+\sqrt{(k+1)^2-4kq}}{2}, 0)$ is an unstable focus or node;
- (6) If $\lambda_5 < 0$, $\lambda_6 < 0$, $E_{02}(\frac{-1+k+\sqrt{(k+1)^2-4kq}}{2},0)$ is a stable focus or node.

Next, we consider stability and type of the positive equilibria of model (2). The Jacobian matrix of model (2) at a positive equilibria E(x,y) is given

(13)

C. Y. Liang et al.

by

$$J(E) = \begin{bmatrix} -\frac{2x}{k} - \frac{py}{(x+1-m)^2} - \frac{q}{(x+1)^2} + 1 & \frac{p(m-x)}{x+1-m} \\ \frac{ay}{(x+1-m)^2} - \frac{by}{k} & 0 \end{bmatrix}.$$
 (14)

The determinant of J(E) is

$$\det(J(E)) = \frac{x[x^2 + (1-k)x + (q-1)][b(-m+x+1)^2 - ak]}{k^2(x+1)(-m+x+1)^2}$$
(15)

and its sign is determined by

$$S_D(x) = [x^2 + (1-k)x + (q-1)][b(-m+x+1)^2 - ak].$$
(16)

The trace of J(E) is

$$\operatorname{tr}(J(E)) = -\frac{2x}{k} - \frac{py}{(-m+x+1)^2} - \frac{q}{(x+1)^2} + 1 \tag{17}$$

and its sign is determined by

$$S_T(x) = \frac{-2x^5 + (k + 4m - 5)x^4 + d_1x^3 + d_2x^2 + d_3x + d_4}{k(x+1)^2(m-x-1)(m-x)},$$
(18)

where

$$d_1 = -2km + 2k - 2m^2 + 10m - 4,$$

$$d_2 = km^2 - 5km + k - 4m^2 + 8m - 1,$$

$$d_3 = (2k - 2)m^2 + m(2kq - 4k + 2),$$

$$d_4 = (m^2 - m)(k - kq).$$

To discuss the topological type of the positive equilibria of model (2), we let

$$q_* = \frac{(k(a+b-c) + \sqrt{a}\sqrt{b}\sqrt{k} + b)^2(2a^{3/2}\sqrt{b}\sqrt{k} + a^2k + ab + ck(b-c))}{b^2k(a+b-c)(k(a+b-c) + 2\sqrt{a}\sqrt{b}\sqrt{k} + b)}.$$
 (19)

Theorem 4. When $m = m_*$ and 0 < k(a + b - c) + b(m - 1) < 2b, model (2) has a unique positive equilibrium $E_*(x_*, y_*)$. Moreover,

- (2) If $q = q_*$, then $E_*(x_*, y_*)$ is a cusp of codimension two.
- (1) If $q \neq q_*$, then $E_*(x_*, y_*)$ is a saddle-node, which is attracting (or repelling) if $q < q_*$ (or $q > q_*$);
- Proof. Substituting x_* and m_1 (m_2 is the same) into S_D and S_T , we deduce that $S_D(x_*) = 0$. Letting $S_T(x_*) = 0$, we have

$$q_* = \frac{(k(a+b-c) + \sqrt{a}\sqrt{b}\sqrt{k} + b)^2(2a^{3/2}\sqrt{b}\sqrt{k} + a^2k + ab + ck(b-c))}{b^2k(a+b-c)(k(a+b-c) + 2\sqrt{a}\sqrt{b}\sqrt{k} + b)}.$$
 (20)

Next, we prove the assertion (2). Let $X = x - x_*$, $Y = y - y_*$, $m = m_2$ and $q = q_*$. Then model (2) is transformed into (we still denote X, Y by x, y, respectively)

$$\frac{dX}{dt} = A_1 Y + A_2 X Y + A_3 X^2 + o(|X, Y|^3), \quad \frac{dY}{dt} = B_1 X^2 + o(|X, Y|^3), \tag{21}$$

where

$$A_{1} = p \left(\frac{\sqrt{b}}{\sqrt{ak}} - 1 \right), \quad A_{2} = -\frac{bp}{ak}, \quad A_{3} = \frac{aA''\sqrt{abk} + A'}{ak(a+b-c)\sqrt{abk}(k(a+b-c) - \sqrt{abk} + b)},$$

$$B_{1} = \frac{\sqrt{a}(\sqrt{k}(a+b-c) - \sqrt{a}\sqrt{b})^{2}(-2\sqrt{abk} + 2ak + bk + b - 2ck)}{kp\sqrt{bk}(a+b-c)(-2\sqrt{abk} + ak + bk + b - ck)}$$

and

$$A' = -ab^{2} - bk(-c(5a + 2b) + (2a + b)^{2} + c^{2})$$
$$-k^{2}(2a + b - 2c)(a + b - c)^{2},$$
$$A'' = 3a^{2}k + ab(5k + 3) - 6ack$$
$$+ (b - c)(2bk + b - 3ck).$$

Letting $d\tau = A_1 dt$, model (21) is transformed into

$$\frac{dX}{d\tau} = Y + \frac{A_2}{A_1}XY + \frac{A_3}{A_1}X^2 + o(|X,Y|^3),
\frac{dY}{d\tau} = \frac{B_1}{A_1}X^2 + o(|X,Y|^3).$$
(22)

By Remark 1 in Sec. 2.13 of Perko, 1996, we obtain an equivalent system of system (22) in the small neighborhood of (0,0) as follows:

$$\frac{dX}{d\tau} = Y + o(|X, Y|^3),$$

$$\frac{dY}{d\tau} = \frac{B_1}{A_1} + \frac{2A_3}{A_1}XY + o(|X, Y|^3) + o(|X, Y|^3).$$
(23)

Then $E_*(x_*, y_*)$ is a cusp of codimension two when $\frac{B_1}{A_1} \neq 0$ and $\frac{2A_3}{A_1} \neq 0$, i.e.

$$b(-k+2m-1) \neq 6\sqrt{abk}$$
 and $a\sqrt{b}k(7k-39m+32) + 36ak\sqrt{ak} + b^{3/2}(m-1)^2(k-2m+1) \neq 5b(m-1)\sqrt{ak}(k-3m+2).$

Theorem 5. When $0 < \frac{k(a+b-c)+b(m-1)}{2b} < 1$, k[(a+b-c)m+2c-2b-a] > bm-2b and (a+b-c)m+c-b>0 are satisfied, model (2) has two positive equilibria $E_1(x_1,y_1)$ and $E_2(x_2,y_2)$ $(x_2 < x_1)$. Moreover, $E_2(x_2,y_2)$ is always a saddle, and $E_1(x_1,y_1)$ is

- (1) a stable focus (or node) if $S_T(x_1) > 0$;
- (2) a unstable focus (or node) if $S_T(x_1) < 0$;
- (3) a center if $S_T(x_1) = 0$.

Here $S_T(x_1)$ is defined in (19).

Proof. The Jacobian matrix of system (2) at E_i (i = 1, 2) is

$$J(E_i) = \begin{bmatrix} -\frac{2x_i}{k} - \frac{py_i}{(x_i - m + 1)^2} - \frac{q}{(x_i + 1)^2} + 1 & \frac{p(x_i - m)}{-x_i + m - 1} \\ \frac{ay_i}{(x_i - m + 1)^2} - \frac{by_i}{k} & 0 \end{bmatrix}.$$
 (24)

Then we can get

$$\det(J(E_i)) = \frac{y_i p(x_i - m)}{x_i + 1 - m} \left(\frac{a}{(x_i + 1 - m)^2} - \frac{b}{k} \right). \tag{25}$$

The sign of $\det(J(E_i))$ is determined by $\frac{a}{(x_i+1-m)^2} - \frac{b}{k}$. Additionally, to determine the types of $E_1(x_1, y_1)$ and $E_2(x_2, y_2)$, we need to consider the signs of $S_D(x_1)$, $S_D(x_2)$ and $S_T(x_1)$.

For

$$S_D(x_1) = -\frac{2b\sqrt{\Delta}}{k(ak+bk-ck+b-bm-\sqrt{\Delta})},$$

we find that $S_D(x_1) > 0$ due to the existence of $E_1(x_1, y_1)$. Thus, if $S_T(x_1) > 0$, $E_1(x_1, y_1)$ is locally asymptotically stable; if $S_T(x_1) < 0$, $E_1(x_1, y_1)$ is unstable.

Similarly, since

$$S_D(x_2) = -\frac{2b\sqrt{\Delta}}{k(ak+bk-ck+b-bm+\sqrt{\Delta})}.$$

we can get that $S_D(x_2) < 0$. Therefore, $E_2(x_2, y_2)$ is a saddle whenever it exists.

3. Bifurcation Analysis

3.1. Saddle-node bifurcation

Lemma 1 (Sotomayor's Theorem Liu & Huang, 2018]). The system $\dot{x} = F(x,m)$ experiences a saddle-node bifurcation at the equilibrium $x_{\rm SN}$ as the control parameter m passes through the bifurcation value $m = m_{\rm SN}$, if the following conditions are satisfied:

$$F_m W^T(E_{SN}; m_{SN}) \neq 0,$$

$$W^T D^2 F_m(E_{SN}; m_{SN})(V, V) \neq 0.$$

According to Theorem \Box , we know that E_1 is locally asymptotically stable if $\operatorname{tr}(J(E_1)) < 0$ and E_2 is a saddle whenever it exists. By controlling the parameter m, the collision of E_1 and E_2 can result in an overlapping equilibrium, denoted as $E_{\rm SN}(x_{\rm SN},y_{\rm SN})$, when $\Delta=0$. As the value of the parameter m changes, the internal equilibria

disappear when $\Delta < 0$. Model (2) undergoes a saddle-node bifurcation at $m = m_{\rm SN}$, where

$$m_{\rm SN} = \frac{k(a+b-c) - 2\sqrt{abk} + b}{b},$$

$$x_{\rm SN} = \frac{k(a+b-c) - \sqrt{abk}}{b},$$

$$y_{\rm SN} = \frac{x_{\rm SN}(x_{\rm SN} - k)(x_{\rm SN} + 1 - m)}{kn(m - x_{\rm SN})}.$$

Theorem 6. Under the condition

$$\max \left\{ b, \frac{k^2(a-c)(a+b-c) + bk(2a+bq-c)}{k(2a+b-2c) + b} \right\}$$

$$< \sqrt{abk} < \frac{1}{2}(k(a+b-c) + b)$$

model (2) undergoes a saddle-node bifurcation at

$$m = m_{\rm SN} \triangleq \frac{k(a+b-c) - 2\sqrt{abk} + b}{b}$$

Proof. When $m = m_{SN} \triangleq \frac{k(a+b-c)-2\sqrt{abk}+b}{b}$, the Jacobian matrix at E_{SN} is as follows:

$$J(E_{\rm SN}) = \begin{bmatrix} 1 - \frac{2x_{\rm SN}}{k} - \frac{py_{\rm SN}}{(x_{\rm SN} + 1 - m)^2} - \frac{q}{(x_{\rm SN} + 1)^2} & -\frac{p(x_{\rm SN} - m)}{x_{\rm SN} + 1 - m} \\ 0 & 0 \end{bmatrix}.$$
(26)

The eigenvectors of the zero eigenvalues of $J_{E_{\rm SN}}$ and $J_{E_{\rm SN}}^T$ are given by:

$$V = \begin{bmatrix} v_1 \\ v_2 \end{bmatrix} = \begin{bmatrix} 1 \\ (-m + x_{\text{SN}} + 1) \left(-\frac{2x_{\text{SN}}}{k} - \frac{py_{\text{SN}}}{(-m + x_{\text{SN}} + 1)^2} - \frac{q}{(x_{\text{SN}} + 1)^2} + 1 \right) \\ p(x_{\text{SN}} - m) \end{bmatrix}, \quad W = \begin{bmatrix} w_1 \\ w_2 \end{bmatrix} = \begin{bmatrix} 0 \\ 1 \end{bmatrix}.$$

Then

 $F_m(E_{\rm SN}; m_{\rm SN})$

$$= \begin{bmatrix} F_{1m} \\ F_{2m} \end{bmatrix} = \begin{bmatrix} \frac{py}{(-m+x+1)^2} \\ -\frac{ay}{(-m+x+1)^2} \end{bmatrix}_{(E_{\text{SN}}; m_{\text{TC}}}$$

$$= \begin{bmatrix} \frac{(\sqrt{k}(a+b-c)-\sqrt{ab})(\sqrt{k}(b(k+1)(a-c)+b(a+bq)+k(a-c)^2)+\sqrt{ab}(2k(c-a)-b(k+1)))}{\sqrt{k}\sqrt{ab}(b-\sqrt{abk})(k(a+b-c)-\sqrt{a}\sqrt{b}\sqrt{k}+b)} \\ -\frac{\sqrt{a}(\sqrt{k}(a+b-c)-\sqrt{ab})(\sqrt{k}(b(k+1)(a-c)+b(a+bq)+k(a-c)^2)+\sqrt{ab}(2k(c-a)-b(k+1)))}{\sqrt{b}\sqrt{k}p(b-\sqrt{abk})(k(a+b-c)-\sqrt{a}\sqrt{b}\sqrt{k}+b)} \end{bmatrix}$$

 $D^2F_m(E_{SN}; m_{SN})(V, V)$

$$= \begin{bmatrix} \frac{\partial^2 F_{1m}}{\partial x^2} v_1^2 + 2 \frac{\partial^2 F_{1m}}{\partial x \partial y} v_1 v_2 + \frac{\partial^2 F_{1m}}{\partial y^2} v_2^2 \\ \frac{\partial^2 F_{2m}}{\partial x^2} v_1^2 + 2 \frac{\partial^2 F_{2m}}{\partial x \partial y} v_1 v_2 + \frac{\partial^2 F_{2m}}{\partial y^2} v_2^2 \end{bmatrix} = \begin{bmatrix} \frac{6py}{(-m+x+1)^4} - \frac{(4p)v_2}{(-m+x+1)^4} - \frac{(4p)v_2}{(-m+x+1)^3} \\ \frac{(4a)v_2}{(-m+x+1)^3} - \frac{6ay}{(-m+x+1)^4} \end{bmatrix}_{(E_{\rm SN}; m_{\rm SN})}$$

 $W^T F_m(E_{\rm SN}; m_{\rm SN})$

$$\begin{split} &= [0,1] \begin{bmatrix} \frac{py}{(-m+x+1)^2} \\ -\frac{ay}{(-m+x+1)^2} \end{bmatrix}_{(E_{\mathrm{SN}};m_{\mathrm{SN}})} \\ &= -\frac{\sqrt{a}(\sqrt{k}(a+b-c)-\sqrt{ab})(\sqrt{k}(b(k+1)(a-c)+b(a+bq)+k(a-c)^2)+\sqrt{ab}(2k(c-a)-b(k+1)))}{\sqrt{b}\sqrt{k}p(b-\sqrt{abk})(k(a+b-c)-\sqrt{a}\sqrt{b}\sqrt{k}+b)} \end{split}$$

 $\neq 0$.

 $W^T D^2 F_m(E_{SN}; m_{SN})(V, V)$

$$= [0,1] \begin{bmatrix} \frac{6py}{(-m+x+1)^4} - \frac{(4p)v_2}{(-m+x+1)^3} \\ \frac{(4a)v_2}{(-m+x+1)^3} - \frac{6ay}{(-m+x+1)^4} \end{bmatrix}_{(E_{\rm SN};m_{\rm SN})} = \frac{(4a)v_2}{(-m+x_{\rm SN}+1)^3} - \frac{6ay_{\rm SN}}{(-m+x_{\rm SN}+1)^4}.$$

According to Lemma \square , model \square undergoes a saddle-node bifurcation around $E_{\rm SN}(x_{\rm SN},y_{\rm SN})$ at $m=m_{\rm SN}$ when $v_2<0$, where

$$v_{2} = \frac{ak}{p(ak - \sqrt{abk})} \left(1 - \frac{b^{2}q}{(k(a+b-c) - \sqrt{abk} + b)^{2}} - \frac{2(k(a+b-c) - \sqrt{abk})}{bk} \right) - \overline{v}_{2}$$

and

$$\overline{v}_2 = \frac{(k(a+b-c) - \sqrt{abk})(k^2(a-c)(a+b-c) + bk(2a+bq-c) - \sqrt{abk}(k(2a+b-2c)+b))}{\sqrt{abk}(b - \sqrt{abk})(k(a+b-c) - \sqrt{abk}+b)}.$$

$3.2. \ Bogdanov-Takens \ bifurcation$

Theorem 7. When $m = m_*$, $q = q_*$, $b(-k+2m-1)-6\sqrt{abk} \neq 0$ and $36a^{3/2}k^{3/2}-5\sqrt{ab}\sqrt{k}(m-1)(k-3m+2)+a\sqrt{bk}(7k-39m+32)+b^{3/2}(m-1)^2(k-2m+1) \neq 0$, $E_*(x_*,y_*)$ is a cusp of codimension two. If we choose m and q as bifurcation parameters, then model (2) undergoes Bogdanov-Takens bifurcation of codimension two in a small neighborhood of the unique positive equilibrium $E_*(x_*,y_*)$.

Proof. Consider

$$\frac{dx}{dt} = x\left(1 - \frac{x}{k}\right) - \frac{py(x - \lambda_2 - m)}{x + 1 - \lambda_2 - m} - \frac{x(\lambda_1 + q)}{x + 1},$$

$$\frac{dy}{dt} = \frac{ay(x - \lambda_2 - m)}{x + 1 - \lambda_2 - m} + by\left(1 - \frac{x}{k}\right) - cy,$$
(27)

where $\lambda = (\lambda_1, \lambda_2) \sim (0, 0)$.

Let $u = x - x_*$, $v = y - y_*$. Then model (27) can be rewritten as

$$\frac{du}{dt} = \alpha_1 + \alpha_2 u + \alpha_3 v + \alpha_4 u^2 + \alpha_5 u v,$$

$$\frac{dv}{dt} = \beta_1 + \beta_2 u + \beta_3 v + \beta_4 u^2 + \beta_5 u v$$

$$+ P_1(u, v, \lambda_1, \lambda_2),$$
(28)

where

$$\alpha_{1} = x_{*} \left(1 - \frac{x_{*}}{k}\right) - \frac{py_{*}(\lambda_{2} + m - x_{*})}{\lambda_{2} + m - x_{*} - 1}$$

$$- \frac{x_{*}(\lambda_{1} + q)}{x_{*} + 1},$$

$$\alpha_{2} = -\frac{2x_{*}}{k} - \frac{py_{*}}{(\lambda_{2} + m - x_{*} - 1)^{2}}$$

$$+ \frac{-\lambda_{1} - q}{(x_{*} + 1)^{2}} + 1,$$

$$\alpha_{3} = -\frac{p(\lambda_{2} + m - x_{*})}{\lambda_{2} + m - x_{*} - 1},$$

$$\alpha_{4} = -\frac{1}{k} - \frac{py_{*}}{(\lambda_{2} + m - x_{*} - 1)^{3}} + \frac{\lambda_{1} + q}{(x_{*} + 1)^{3}},$$

$$\alpha_{5} = -\frac{p}{(\lambda_{2} + m - x_{*} - 1)^{2}},$$

$$\beta_{1} = \frac{ay_{*}(\lambda_{2} + m - x_{*})}{\lambda_{2} + m - x_{*} - 1} + by_{*} \left(1 - \frac{x_{*}}{k}\right) - cy_{*},$$

$$\beta_{2} = \frac{ay_{*}}{(\lambda_{2} + m - x_{*} - 1)^{2}} - \frac{by_{*}}{k},$$

$$\beta_{3} = \frac{a(\lambda_{2} + m - x_{*})}{\lambda_{2} + m - x_{*} - 1} + b\left(1 - \frac{x_{*}}{k}\right) - c,$$

$$\beta_{4} = \frac{ay_{*}}{(\lambda_{2} + m - x_{*} - 1)^{3}},$$

$$\beta_{5} = \frac{a}{(\lambda_{2} + m - x_{*} - 1)^{2}} - \frac{b}{k},$$

 $P_1(u, v, \lambda_1, \lambda_2)$ is a power series in (u, v) with terms $u^i v^j$ satisfying $i + j \geq 3$, and the coefficients depend smoothly on λ_1 and λ_2 .

Let $n_1 = u$, $n_2 = \alpha_1 + \alpha_2 u + \alpha_3 v + \alpha_4 u^2 + \alpha_5 uv$. The model (28) becomes

$$\frac{dn_1}{dt} = n_2,$$

$$\frac{dn_2}{dt} = \xi_1 + \xi_2 n_1 + \xi_3 n_2 + \xi_4 n_1^2 + \xi_5 n_1 n_2$$

$$+ \xi_6 n_2^2 + P_2(n_1, n_2, \lambda_1, \lambda_2),$$
(29)

where

$$\xi_1 = \alpha_3 \beta_1 - \alpha_1 \beta_3,$$

$$\xi_2 = \alpha_5 \beta_1 + \alpha_3 \beta_2 - \alpha_2 \beta_3 - \alpha_1 \beta_5,$$

$$\xi_3 = \alpha_2 - \frac{\alpha_1 \alpha_5}{\alpha_3} + \beta_3,$$

$$\xi_4 = \alpha_5 \beta_2 - \alpha_4 \beta_3 + \alpha_3 \beta_4 - \alpha_2 \beta_5,$$

$$\xi_5 = \frac{\alpha_3^2 \beta_5 + 2\alpha_4 \alpha_3^2 - \alpha_2 \alpha_5 \alpha_3 + \alpha_1 \alpha_5^2}{\alpha_3^2},$$

$$\xi_6 = \frac{\alpha_5}{\alpha_3}$$

and $P_2(n_1, n_2, \lambda_1, \lambda_2)$ is a power series in (n_1, n_2) with terms $n_1^i n_2^j$ satisfying $i + j \geq 3$, and the coefficients depend smoothly on λ_1 and λ_2 .

Let $dt = d\tau (1 - \xi_6 n_1)$. Then model (29) becomes

$$\frac{dn_1}{d\tau} = n_2(1 - \xi_6 n_1),$$

$$\frac{dn_2}{d\tau} = 1 - \xi_6 n_1(\xi_1 + \xi_2 n_1 + \xi_3 n_2 + \xi_4 n_1^2 + \xi_5 n_1 n_2 + \xi_6 n_2^2 + P_2(n_1, n_2, \lambda_1, \lambda_2)).$$
(30)

Letting $z_1 = n_1, z_2 = n_2(1 - \xi_6 n_1)$, we obtain

$$\frac{dz_1}{d\tau} = z_2,
\frac{dz_2}{d\tau} = \eta_1 + \eta_2 z_1 + \eta_3 z_2 + \eta_4 z_1^2 + \eta_5 z_1 z_2
+ P_3(z_1, z_2, \lambda_1, \lambda_2),$$
(31)

where

$$\eta_1 = \xi_1, \quad \eta_2 = \xi_2 - 2\xi_1 \xi_6, \quad \eta_3 = \xi_3,
\eta_4 = \xi_1 \xi_6^2 - 2\xi_2 \xi_6 + \xi_4, \quad \eta_5 = \xi_5 - \xi_3 \xi_6$$

and $P_3(z_1, z_2, \lambda_1, \lambda_2)$ is a power series in (z_1, z_2) with terms $z_1^i z_2^j$ satisfying $i + j \geq 3$, and the coefficients depend smoothly on λ_1 and λ_2 .

When $\eta_4 > 0$, we let $u_1 = z_1$, $u_2 = \frac{z_2}{\sqrt{\eta_4}}$, $\tau_1 = \sqrt{\eta_4}\tau$. Then model (31) can be written as

$$\frac{du_1}{d\tau_1} = u_2,$$

$$\frac{du_2}{d\tau_2} = \theta_1 + \theta_2 u_1 + \theta_3 u_2 + u_1^2 + \theta_4 u_1 u_2 + P_4(u_1, u_2, \lambda_1, \lambda_2),$$
(32)

where

$$\theta_1 = \frac{\eta_1}{\eta_4}, \quad \theta_2 = \frac{\eta_2}{\eta_4}, \quad \theta_3 = \frac{\eta_3}{\sqrt{\eta_4}}, \quad \theta_4 = \frac{\eta_5}{\sqrt{\eta_4}}$$

and $P_4(u_1, u_2, \lambda_1, \lambda_2)$ is a power series in (u_1, u_2) with terms $u_1^i u_2^j$ satisfying $i + j \geq 3$, and the coefficients depend smoothly on λ_1 and λ_2 .

Further, letting

$$\omega_1 = \frac{\theta_2}{2} + u_1, \quad \omega_2 = u_2,$$

model (32) can be written as

$$\frac{d\omega_1}{d\tau_1} = \omega_2,$$

$$\frac{d\omega_2}{d\tau_2} = \gamma_1 + \gamma_2\omega_2 + \omega_1^2 + \gamma_3\omega_1\omega_2$$

$$+ P_5(\omega_1, \omega_2, \lambda_1, \lambda_2),$$
(33)

where

$$\gamma_1=\theta_1-\frac{\theta_2^2}{4},\quad \gamma_2=\theta_3-\frac{\theta_2\theta_4}{2},\quad \gamma_3=\theta_4$$

and $P_5(\omega_1, \omega_2, \lambda_1, \lambda_2)$ is a power series in (ω_1, ω_2) with terms $\omega_1^i \omega_2^j$ satisfying $i + j \geq 3$, and the coefficients depend smoothly on λ_1 and λ_2 .

Making the final change of variables by setting

$$x = \gamma_3^2 \omega_1, \quad y = \gamma_3^3 \omega_1, \quad \tau = \frac{\tau_1}{\gamma_3},$$

we finally obtain

$$\frac{dx}{d\tau} = y,$$

$$\frac{dy}{d\tau} = \zeta_1 + \zeta_2 y + x^2 + xy + P_6(x, y, \lambda_1, \lambda_2),$$
(34)

where

$$\zeta_1 = \gamma_1 \gamma_3^4, \quad \zeta_2 = \gamma_2 \gamma_3$$

and $P_6(x, y, \lambda_1, \lambda_2)$ is a power series in (x, y) with terms $x^i y^j$ satisfying $i + j \geq 3$, and the coefficients depend smoothly on λ_1 and λ_2 .

We can express ζ_1 and ζ_2 in terms of λ_1 and λ_2 as follows:

$$\zeta_{1} = \lambda_{1}s_{1} + \lambda_{2}s_{2} + \lambda_{1}^{2}s_{3} + \lambda_{1}\lambda_{2}s_{4}
+ \lambda_{2}^{2}s_{5} + o(|(\lambda_{1}, \lambda_{2})|),
\zeta_{2} = \lambda_{1}t_{1} + \lambda_{2}t_{2} + \lambda_{1}^{2}t_{3} + \lambda_{1}\lambda_{2}t_{4}
+ \lambda_{2}^{2}t_{5} + o(|(\lambda_{1}, \lambda_{2})|).$$
(35)

Then

$$\left| \frac{\partial(\zeta_1, \zeta_2)}{\partial(\lambda_1, \lambda_2)} \right| = -\frac{32\rho_1^4(ab^2 + k^2(a+b-c)^2(2a+b-2c) + \rho_2\sqrt{abk} + bk\rho_3)^5}{a^2\rho_1^6\rho_5^8\rho_6^6(a+b-c)\sqrt{abk}(\sqrt{b} - \sqrt{ak})^4},$$

where

$$\begin{split} \rho_1 &= k(a+b-c) - 2\sqrt{abk} + b, \\ \rho_2 &= -ab(5k+3) + ak(6c-3a) - ((b-c)(k(2b-3c)+b)), \\ \rho_3 &= c(-5a-2b+c) + (2a+b)^2, \\ \rho_4 &= \sqrt{k}(a+b-c) - \sqrt{ab}, \\ \rho_5 &= k(2a+b-2c) - 2\sqrt{abk} + b, \\ \rho_6 &= k(a+b-c) - \sqrt{abk} + b. \end{split}$$

Only when

$$c \neq \frac{-bk(b(k-1)^2 - 9ak) - 3\sqrt{abk} + 6ak + 5bk + b}{12k\sqrt[3]{3\sqrt{3}\sqrt{ab^3k^7\rho_7} + 27ab^2(k-1)k^4 + 54abk^4\sqrt{abk} + b^3(k-1)^3k^3}},$$

where

$$\rho_7 = 135a^2k^2 + 18ab(k-1)^2k + 4b(k-1)^3\sqrt{abk} + 108a(k-1)k\sqrt{abk} + 3b^2(k-1)^4,$$

we have

$$\left| \frac{\partial(\zeta_1, \zeta_2)}{\partial(\lambda_1, \lambda_2)} \right| \neq 0.$$

Model (2) undergoes a Bogdanov-Takens bifurcation of codimension two when $\lambda = (\lambda_1, \lambda_2)$ is in a small neighborhood of the origin.

3.3. Hopf bifurcation

Firstly, letting

$$dt = k^2 p(x+1)(x+1-m)(m-x_1)(x_1+1)d\tau,$$

we obtain

$$\frac{dx}{d\tau} = kp(x_1+1)(m-x_1)[kp(x+1)y(m-x)
+ x(m-x-1)(k(q-x-1)+x^2+x)],
\frac{dy}{d\tau} = -kpy(x+1)(x_1+1)(x_1-m)[ak(m-x)
+ b(k-x)(m-x-1) + ck(-m+x+1)].$$
(36)

Noticing that

$$y_1 = \frac{x_1(-m + x_1 + 1)(k(q - x_1 - 1) + x_1^2 + x_1)}{kp(x_1 + 1)(m - x_1)},$$

$$\begin{split} q_1 &= \frac{kq - kx_1 - k + x_1^2 + x_1}{x_1^2}, \\ q_2 &= \frac{-kx_1\overline{x} + x_1^2\overline{x}^2 + x_1\overline{x} + kq - k}{x_1^2}, \\ q_3 &= \frac{x_1\overline{x}(bx_1\overline{x} + k(c-a) - b(k+m-1)) + k(m(a+b-c) - b + c)}{x_1^2} \end{split}$$

Then taking the parameter scaling as follows:

$$\overline{a} = \frac{a}{x_1}, \quad \overline{b} = \frac{b}{x_1}, \quad \overline{c} = \frac{c}{x_1}, \quad \overline{m} = \frac{m}{x_1},$$

$$\overline{k} = \frac{k}{x_1}, \quad \overline{q} = \frac{q}{x_1}, \quad g = \frac{1}{x_1},$$

after dropping the bars, we obtain

$$\frac{dx}{dt} = \frac{kp}{g} [q_4 y (g - m + 1)(g + x)(m - x) + q_5 (g + 1)(m - 1)x(-g + m - x)],$$

$$\frac{dy}{dt} = \frac{q_6 kpy}{g} (g + 1)(1 - m)(g + x),$$

we use the following scalings of the coordinates,

$$\bar{x} = \frac{x}{x_1}, \quad \bar{y} = \frac{y}{y_1}, \quad \tau = \frac{t}{x_1^5},$$
 (37)

under which model (2) is transformed to

$$\frac{d\overline{x}}{dt} = \frac{kp}{x_1^3} [q_1 \overline{y}(x_1 \overline{x} + 1)(-m + x_1 + 1)(m - x_1 \overline{x}) - q_2 \overline{x}(x_1 + 1)(m - x_1)(x_1 \overline{x} - m + 1)],$$

$$\frac{d\overline{y}}{dt} = -\frac{q_3 k p \overline{y}}{x_1^3} (x_1 + 1)(x_1 \overline{x} + 1)(m - x_1),$$
(38)

where

where

 $q_{5} + 1 = -gk + gx + kq - kx + x^{2},$ $q_{6} = \frac{km(a+b-c) - kx(a+b-c) - bmx + bx^{2}}{a}$

-bk + bx + ck.

 $a_A = a(-k) + a + ka - k$

Since model (39) has an equilibrium $\tilde{E}_1(1,1)$ (i.e. $E_1(x_1,y_1)$ of model (2), we have

$$k = \frac{b(g - m + 1)}{(1 - m)(a + b - c) + g(b - c)},$$

which is then substituted into (39) to finally yield the following model

$$\frac{dx}{dt} = \frac{bp(-q_7 + q_8 - q_9)(g - m + 1)}{g[a - am + (b - c)(g - m + 1)]^2},$$

$$\frac{dy}{dt} = \frac{b^2 py(g + 1)(1 - m)(q_{10} + q_{11})(x - 1)(g - m + 1)(g + x)}{g^2[a - am + (b - c)(g - m + 1)]^2},$$
(40)

where

$$q_7 = x^2(g+1)(1-m)(g+x)(g-m+x)[a(m-1)+c(g-m+1)],$$

$$q_8 = b(g-m+1)[g(x-1)+q+(x-1)x],$$

$$q_9 = y(g-m+1)(g+x)(m-x)[a(g+1)(m-1)+(g-m+1)(-bq+cg+c)].$$

(39)

In the following, we study the Hopf bifurcation around $\tilde{E}_1(1,1)$ in model (\square), which corresponds to the Hopf bifurcation around $E_1(x_1,y_1)$ in model (\square).

Theorem 8. Model (40) has an equilibrium at $\tilde{E}_1(1,1)$. Moreover,

- (1) when $q = q^+$, $\tilde{E}_1(1,1)$ is a focus or center;
- (2) when $q > q^+$, $\tilde{E}_1(1,1)$ is a locally asymptotically stable hyperbolic node or focus;

(3) when $q < q^+$, $\tilde{E}_1(1,1)$ is an unstable hyperbolic node or focus.

Proof. The Jacobian matrix of model (40) at $\tilde{E}_1(1,1)$ is

$$J(\tilde{E}_1(1,1)) = \begin{bmatrix} a_{11} & a_{12} \\ a_{21} & 0 \end{bmatrix}, \tag{41}$$

where

$$a_{11} = \frac{bp(q_{10} - q_{11})(g - m + 1)}{g[a - am + (b - c)(g - m + 1)]^2},$$

$$a_{12} = -\frac{bp(g + 1)(m - 1)(g - m + 1)^2[a(g + 1)(m - 1) + (g - m + 1)(-bq + cg + c)]}{g[a(1 - m) + (b - c)(g - m + 1)]^2},$$

$$a_{21} = -\frac{b^2p(g + 1)^2(m - 1)(g - m + 1)[a(m^2 + 1) - (g + 2)am + (b - c)(g - m + 1)^2]}{g^2[a(1 - m) + (b - c)(g - m + 1)]^2}$$

and

$$q_{10} = a(g+1)^{2}(m-1)[g(2m-1) - 2(m-1)^{2}],$$

$$q_{11} = (g-m+1)[(g+1)^{2}(b(m-1)(g-m+1) + c(-2(g+2)m + g + 2m^{2} + 2)) + bgmq(g-m+2)].$$

The determinant of $J(\tilde{E}_1(1,1))$ is

$$\det(J(\tilde{E}_1))$$

$$=\frac{b^3p^2q_{12}q_{13}(g+1)^3(m-1)^2(g-m+1)^3}{g^3[a-am+(b-c)(g-m+1)]^4},$$

where

$$q_{12} = a[-(g+2)m + m^2 + 1] + (b-c)(g-m+1)^2,$$

$$q_{13} = a(g+1)(1-m) - (g-m+1)(-bq + cg + c)$$

and the trace of $J(\tilde{E}_1(1,1))$ is

$$tr(J(\tilde{E}_1)) = a_{11}$$

$$= \frac{bp(q_{10} - q_{11})(g - m + 1)}{g[a - am + (b - c)(g - m + 1)]^2}.$$

We can see that $\det(J(\tilde{E}_1)) > 0$ and $\operatorname{tr}(J(\tilde{E}_1)) = 0$ if $q = q^+$, where

$$q^{+} = -\frac{(g+1)^{2} \{a(m-1)(-2gm+g+2(m-1)^{2}) + (g-m+1)(b(m-1)(g-m+1) + c(-2(g+2)m+g+2m^{2}+2))\}}{bgm(g-m+1)(g-m+2)}$$

The leads to the conclusions.

Next, we check the transversality condition

$$\left. \frac{d}{dq} \operatorname{tr}(J) \right|_{q=q^+} = -\frac{b^2 m p (g-m+1)^2 (g-m+2)}{[a(1-m) + (b-c)(g-m+1)]^2} < 0.$$

Let u = x - 1, v = y - 1 and $q = q_+$. Model (40) can be written as

$$\frac{du}{dt} = a_1v + a_2u^2 + a_3uv + a_4u^3 + a_5u^2v, \quad \frac{dv}{dt} = b_1u + b_2u^2 + b_3uv + b_4u^3 + b_5u^2v, \tag{42}$$

where

$$a_1 = \frac{(g+1)k(m-1)p(g-m+1)(g(-k)+g+kq-k+1)}{q},$$

$$\begin{split} &kp((-g+m-1)(g(-k)+g+kq-k+1)+(g+1)(m-1)((g-k+2)(-g+m-2)\\ &+gk-2g-kq+k+m-2))\\ &g\\ &\\ &a_3 = \frac{kp(g-m+1)(-g+m-2)(g(-k)+g+kq-k+1)}{g},\\ &a_4 = \frac{(g+1)k(m-1)p(-2g+k+m-4)}{g},\\ &a_5 = \frac{b(g+1)(m-1)p(g-m+1)^3((g-m+1)(b(g+1)-c(g+2))-a(g+2)(m-1))}{g^2m(g-m+2)(a(-m)+a+(b-c)(g-m+1))^2},\\ &b_1 = \frac{(g+1)k(m-1)p((g+1)(k(a-c)+b(-g+k+m-2))+k(-a(m-1)-c(g-m+1))}{g^2}\\ &b_2 = \frac{(g+1)k(m-1)p(k(a-c)+b(-g+k+m-2)-b(g+1))}{g^2},\\ &b_2 = \frac{(g+1)k(m-1)p(k(a-c)+b(-g+k+m-2))+k(-a(m-1)-c(g-m+1))}{g^2}\\ &b_4 = -\frac{b(g+1)k(m-1)p}{g^2},\\ &b_5 = \frac{(g+1)k(m-1)p(k(a-c)+b(-g+k+m-2)-b(g+1))}{g^2}. \end{split}$$

Let

$$\omega = \frac{(g+1)Gk(m-1)p(g-m+1)(g(1-k)+kq-k+1)}{g}$$

and make transformations of u = X, v = GY and $dt = \frac{d\tau}{\omega}$, where

$$G = \frac{(g+1)\sqrt{(m-1)(g-m+1)}\sqrt{-bm(-g+m-2)(a(-(g+2)m+m^2+1)+(b-c)(g-m+1)^2)}}{\sqrt{(g+1)^2(m-1)^2(g-m+1)^3(a(g+2)(m-1)-(g-m+1)(b(g+1)-c(g+2)))}}$$

Model (42) becomes

$$\frac{dx}{dt} = y + f(x,y), \quad \frac{dy}{dt} = -x + g(x,y), \tag{43}$$

where

$$f(x,y) = \tilde{a}_{21}x^2y + \tilde{a}_{30}x^3 + \tilde{a}_{20}x^2 + \tilde{a}_{12}xy^2 + \tilde{a}_{11}xy + \tilde{a}_2y^2 + \tilde{a}_3y^3,$$

$$g(x,y) = \tilde{b}_{21}x^2y + \tilde{b}_{30}x^3 + \tilde{b}_{20}x^2 + \tilde{b}_{12}xy^2 + \tilde{b}_{11}xy + \tilde{b}_2y^2 + \tilde{b}_3y^3$$

and

$$\tilde{a}_{20} = \frac{(g-k+2)(-g+m-2) + (g+1)(k-2) - kq + m}{G(g-m+1)(g(-k) + g + kq - k + 1)} + \frac{1}{(g+1)G(1-m)},$$

$$\tilde{a}_{11} = \frac{-g+m-2}{(g+1)(m-1)},$$

$$\begin{split} \tilde{a}_{30} &= \frac{-2g+k+m-4}{G(g-m+1)(g(-k)+g+kq-k+1)}, \\ \tilde{a}_{21} &= \frac{b(g-m+1)^2((g-m+1)(b(g+1)-c(g+2))-a(g+2)(m-1))}{gkm(g-m+2)(g(-k)+g+kq-k+1)(a(-m)+a+(b-c)(g-m+1))^2}, \\ \tilde{b}_{20} &= \frac{ak-2bg+bk+bm-3b-ck}{gG^2(g-m+1)(gk-g-kq+k-1)}, \\ \tilde{b}_{11} &= -\frac{(g+1)(k(a-c)+b(-g+k+m-2))+k(-a(m-1)-c(g-m+1))+b(k-1)(g-m+1)}{gG(g-m+1)(g(-k)+g+kq-k+1)}, \\ \tilde{b}_{30} &= \frac{b}{gG^2(g-m+1)(g(-k)+g+kq-k+1)}, \\ \tilde{b}_{21} &= \frac{ak-2bg+bk+bm-3b-ck}{gG(g-m+1)(gk-g-kq+k-1)}, \quad \tilde{a}_{02} &= \tilde{a}_{12} = \tilde{a}_{03} = \tilde{b}_{02} = \tilde{b}_{12} = \tilde{b}_{03} = 0. \end{split}$$

We obtain the first Lyapunov coefficient as follows:

$$\sigma_1 = \frac{(\tilde{a}_{20}(2\tilde{b}_{20} - \tilde{a}_{11}) + 3\tilde{a}_{30} + \tilde{b}_{11}\tilde{b}_{20} + \tilde{b}_{21})}{8}$$

$$= \frac{bm^2(g - m + 2)^2(M_2(g + 1)^2(m - 1)^2(g - m + 1)^3)^{3/2}(a^2\varphi_3 + a\varphi_2 + \varphi_1)}{8M_2^2M_1^{3/2}(g + 1)^5(m - 1)^3(g - m + 1)^4((m - 1)(g - m + 1))^{3/2}},$$

where

$$\varphi_{1} = (g+1)(m-1)M_{3}(b-c)(g-m+1)^{3} - \frac{gM_{4}M_{6}(b-c)(g-m+1)^{2}}{g-m+2},$$

$$\varphi_{2} = \frac{g(g-m+1)((m-1)M_{6}M_{7}(b-c) + M_{8}(M_{11}-cM_{7}))}{g-m+2} + (g+1)(m-1)(g-m+1)$$

$$\times (M_{5}(b-c) - 3gM_{10}),$$

$$\varphi_{3} = (g+1)(m-1)M_{9}(-(g+2)m+m^{2}+1) - \frac{g(m-1)M_{7}M_{8}}{g-m+2}$$

$$M_{1} = bm(g - m + 2)(a(-(g + 2)m + m^{2} + 1) + (b - c)(g - m + 1)^{2}),$$

$$M_{2} = a(g + 2)(m - 1) + (g - m + 1)(b(g + 1) - c(g + 2)),$$

$$M_{3} = 2b(b - c)(2g - m + 2) + (g - 2g + m - 4)),$$

$$M_{4} = bb(g^{3} + 5g^{2} + (g + 2)m^{2} + (g + 2)(2g + 3)m + 9g + 5) - cM_{7},$$

$$M_{5} = 2bM_{12} + 3g(m - 1)(g - m + 1) + (g - 2g + m - 4),$$

$$M_{6} = 2gm + (g - 1)g - m^{2} + 3m - 2,$$

$$M_{7} = (g + 3)m^{2} - (g + 3)(2g + 3)m + (g + 2)^{3},$$

$$M_{8} = g^{2}m + 2g(m - 1)m + g$$

$$- (m - 2)(m - 1)^{2},$$

$$M_{9} = 2b(-2gm + g + m^{2} - 3m + 2) + 3g(m - 1)(2g - m + 4),$$

$$M_{10} = (-(g + 2)m + m^{2} + 1)(b(2g - m + 3) + c(-2g + m - 4)),$$

$$M_{11} = b(g^{3} + 5g^{2} + (g + 2)m^{2} + (g + 2)m^{2} + (g + 2)(2g + 3)m + 9g + 5),$$

$$M_{12} = g^{2}(1 - 4m) + g(6(m - 2)m + 5) + (g - 2)(m - 1)^{2}.$$

We can determine the sign of M_1 and M_2 , both of which are positive. Therefore, we only need to determine the sign of the expression $\phi = a^2 \varphi_3 + a\varphi_2 + \varphi_1$.

If $\phi > 0$ (i.e. $\sigma_1 > 0$), model (40) exhibits a supercritical Hopf bifurcation, and a stable limit cycle appears around $\tilde{E}_1(1,1)$. If $\phi < 0$ (i.e. $\sigma_1 < 0$), model (40) exhibits a subcritical Hopf bifurcation, and an unstable limit cycle appears around $\tilde{E}_1(1,1)$. If $\phi = 0$ (i.e. $\sigma_1 = 0$), model (40) may exhibit a degenerate Hopf bifurcation, and multiple limit cycles may appear around $\tilde{E}_1(1,1)$.

4. Numerical Simulations

To illustrate the obtained results, we conducted numerical simulations using Auto07 [Doedel & Oldeman, 2007] with the parameter values employed in [Li et al., 2021], as follows:

$$a = 0.6, \quad b = 0.2, \quad c = 0.55,$$

 $k = 15, \quad m = 1.9, \quad p = 1, \quad q = 0.5.$ (44)

4.1. m, q and k as primary bifurcation parameters

Firstly, if we consider the aggregation effect of Microcystis aeruginosa (m) as the bifurcation parameter, we observe the following bifurcation points: At m = 6.33359, there is a saddlenode bifurcation point $SN(1.20418 \times 10^{-1}, 2.24830)$; At m = 2.21613, we have a supercritical Hopf bifurcation point HB(4.33867, 3.93880); A quasitranscritical bifurcation point QTC(14.4529,0) occurs at m = 4.88623. Furthermore, there exists a family of stable limit cycles approaching a heteroclinic cycle that connects the equilibria (0,0) and (14.5166, 0). It is important to note that the aggregation effect of Microcystis aeruginosa may ultimately lead to the extinction of both Microcystis aeruginosa and filter-feeding fish. For more detailed information, refer to Figs. $\Pi(a)$ – $\Pi(c)$.

Secondly, if we consider b=0.3 and the maximum harvesting rate of Microcystis aeruginosa (q) as the bifurcation parameter, we observe the following bifurcation points: At q=1.72752, there is a supercritical Hopf bifurcation point HB(2.96382, 2.10784); At q=1, there are two transcritical bifurcation points: $TC_1(0,0)$ and $TC_2(2.96382,0)$; At q=4.26667, we have a saddlenode bifurcation point SN(7.0,0). Similar to the previous case, there exists a family of stable limit

cycles approaching a heteroclinic cycle connecting the equilibria (0,0) and (14.5166,0). Please refer to Figs. 2(a)–2(c) for visual representation. Biologically, when the maximum harvesting rate of Microcystis aeruginosa increases, the density of filter-feeding fish also increases. However, there is a critical threshold at q=4.26667, indicating that the filter-feeding fish may go extinct if it exceeds this threshold. It is worth noting that the number of filter-feeding fish starts to decrease when Microcystis aeruginosa is harvested. Hence, finding an appropriate timing for Microcystis aeruginosa harvesting is crucial to promote the number of filter-feeding fish, which may be influenced by the carrying capacity of Microcystis aeruginosa.

Next, we use the maximum environmental capacity of Microcystis aeruginosa (k) as the bifurcation parameter. We observe the following bifurcation points: A transcritical bifurcation point $TC(1.12112 \times 10^{1}, 0)$ at $k = 1.16899 \times 10^{1}$, a saddlenode bifurcation point SN(6.11425, 1.92959) at k =9.06280, and a supercritical Hopf bifurcation point HB(4.15171, 3.45064) at $k = 1.26805 \times 10^{1}$. A family of stable limit cycles bifurcates from the Hopf bifurcation point HB and approaches a homoclinic cycle. Interestingly, the density of filter-feeding fish continues to increase with sustained oscillations as the density of Microcystis aeruginosa increases. This suggests that both populations will coexist with sustainable oscillations. Refer to Figs. (a) and (b) for more details.

4.2. k and a as primary bifurcation parameters

Now, we consider the carrying capacity of Microcystis aeruginosa (k) and the absorption coefficient (a)as the primary bifurcation parameters. As a result, we obtain a two-parameter bifurcation diagram that includes a Hopf bifurcation curve H (red), a saddle-node bifurcation curve SN (green), and a homoclinic bifurcation curve Hom (black). We identify a BT bifurcation point BT(7.49330, 4.37120) at $k = 1.67914 \times 10^{1}, a = 5.17783 \times 10^{-1}, \text{ as well}$ as a codimension-2 cusp point CP(5.38100,0) at $k = 5.83849, a = 6.87827 \times 10^{-1}$. It is noteworthy that despite both parameters k and a being positive, the number of filter-feeding fish will reach zero. In other words, if the carrying capacity is below the threshold of k = 5.83849, the filter-feeding fish will go extinct. Refer to Fig. 4 for a visual representation.

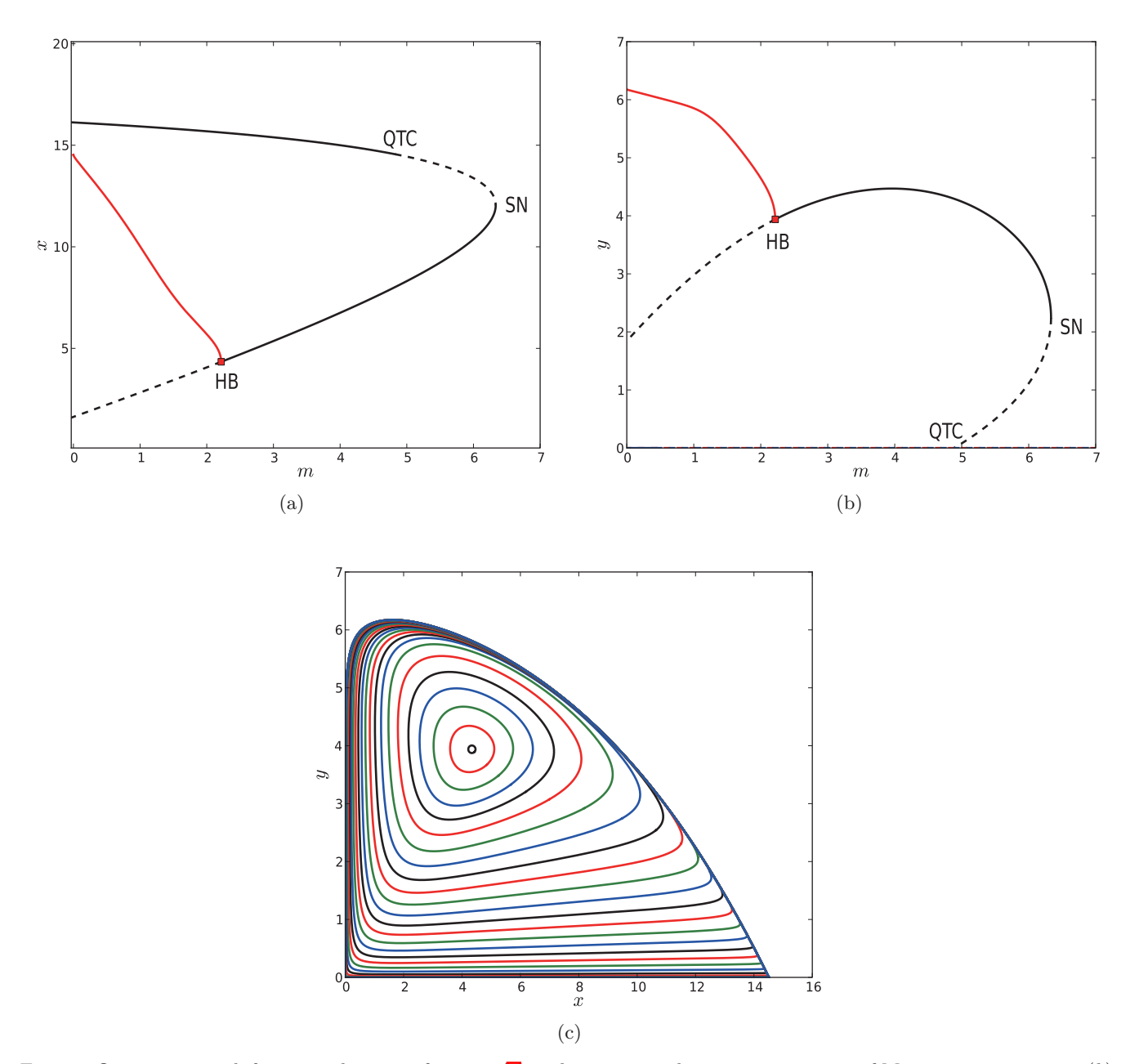


Fig. 1. One-parameter bifurcation diagram of system B with respect to the carrying capacity of Microcystis aeruginosa (k): (a) m versus x; (b) m versus y and (c) a family of limit cycles approaching a heteroclinic cycle.

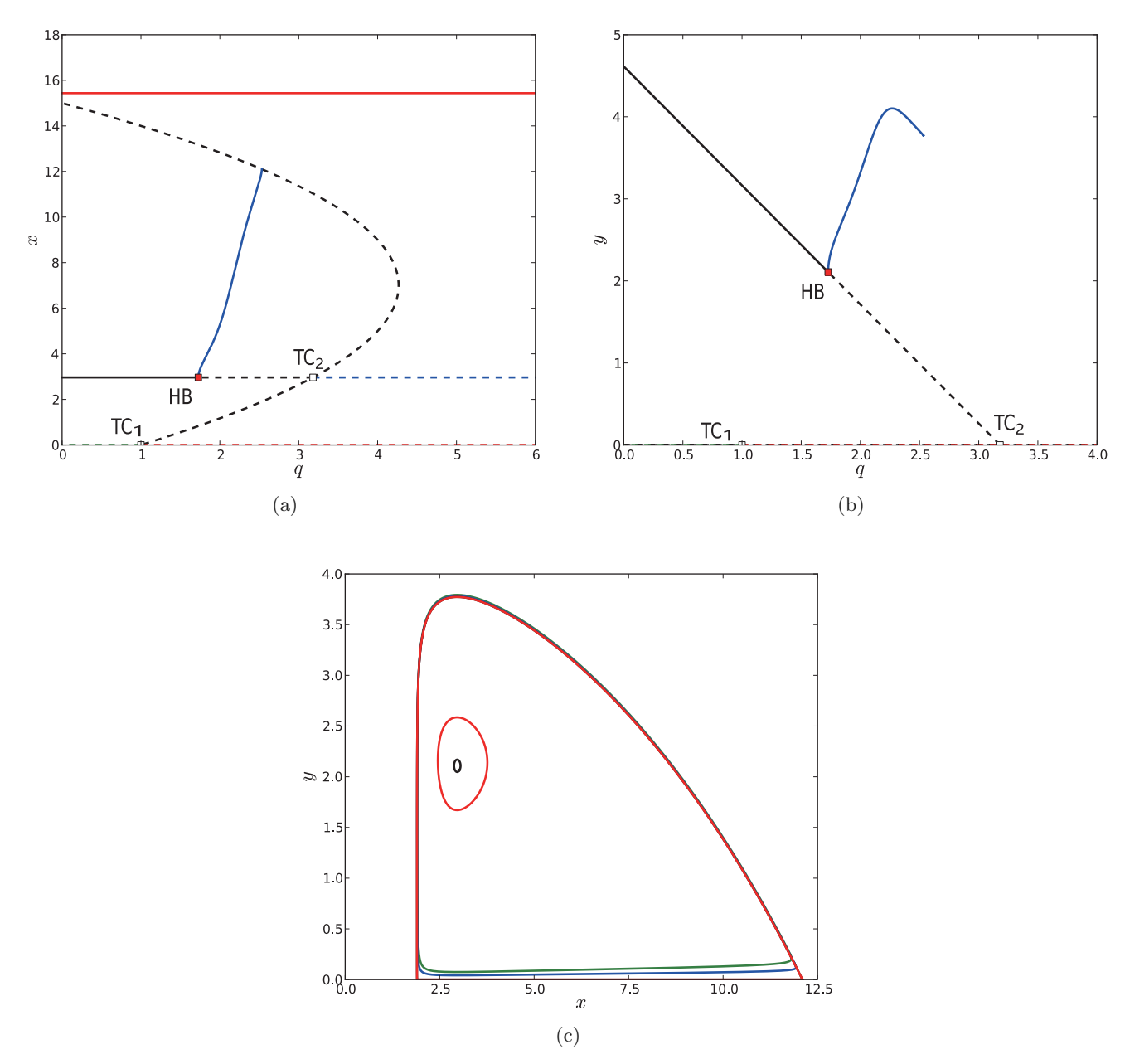
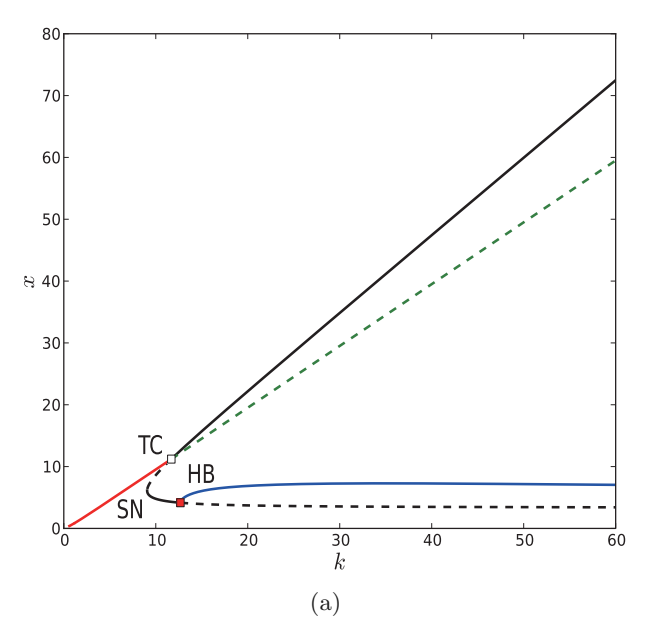


Fig. 2. One-parameter bifurcation diagram of system B with respect to the maximum harvesting rate of Microcystis aeruginosa (q). (a) q versus x; (b) q versus y and (c) a family of limit cycles approaching a heteroclinic cycle.



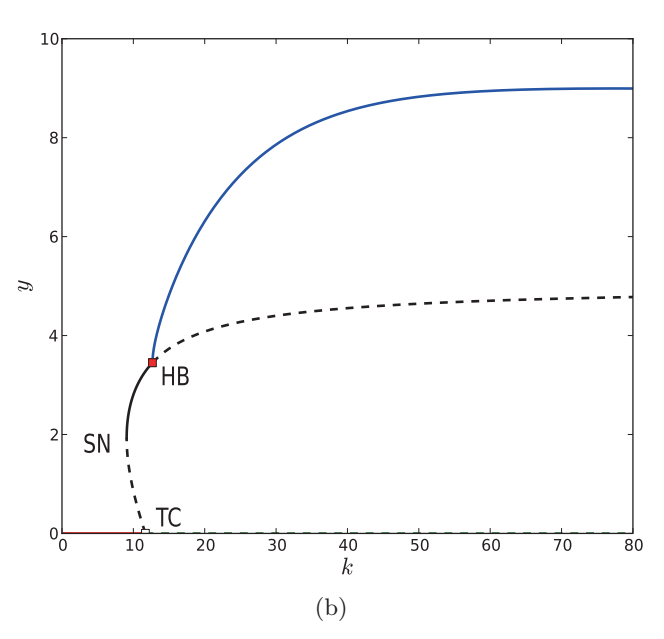


Fig. 3. One-parameter bifurcation diagram of system 3 with respect to the carrying capacity of Microcystis aeruginosa (k). (a) k versus x and (b) k versus y.

The entire phase plane depicted in Fig. 4 is divided into four regions: I–IV. The corresponding phase portraits are as follows:

- (I) a = 0.555752, k = 10.8145: An unstable node at (0,0) and a stable node at (10.3376,0);
- (II) a = 0.564029, k = 12.1542: An unstable node at (0,0), a stable node at (11.6747,0), a stable focus at (5.4149,3.3145), and a saddle at (8.4918,2.4318);

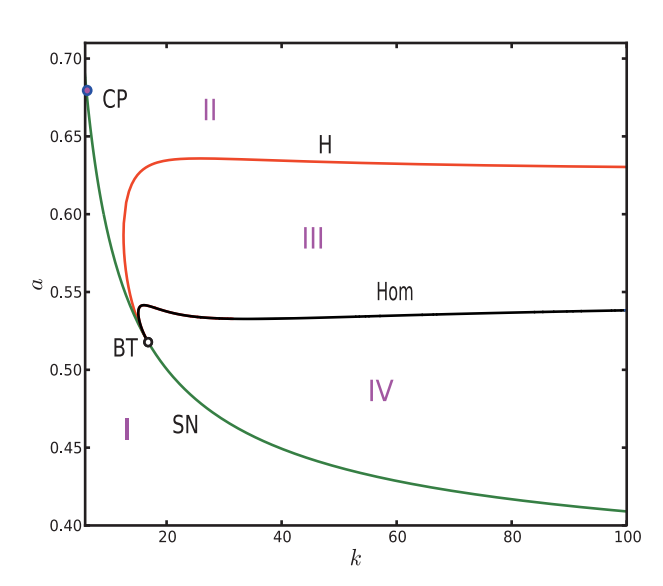


Fig. 4. Two-parameter bifurcation diagram of system 3 with respect to the carrying capacity of Microcystis aeruginosa (k) and the absorption coefficient (a).

- (III) a = 0.632307, k = 19.8129: An unstable node at (0,0), a saddle at (19.3255,0), and a stable limit cycle containing the unstable focus at (3.4555, 4.0498);
- (IV) a = 0.54005089, k = 15.5000905: An unstable node at (0,0), a stable node at (15.0162,0), a homoclinic cycle containing the unstable focus at (5.374,3.9785), and a saddle at (10.2551,3.3754).

When the carrying capacity of Microcystis aeruginosa is small, a large absorption coefficient of the filter-feeding fish cannot guarantee their survival. Similarly, when the carrying capacity of Microcystis aeruginosa is large enough, a small absorption coefficient of the filter-feeding fish may lead to their extinction. In other words, the filter-feeding fish may go extinct whether the carrying capacity of Microcystis aeruginosa is sufficiently small or sufficiently large. Refer to Fig. 5 for a detailed illustration.

It is worth noting that the coexistence of Microcystis aeruginosa and filter-feeding fish occurs when the absorption coefficient is less than a=0.530151 or when the death rate of filter-feeding fish exceeds the threshold of c=0.609115. In other words, as long as the absorption coefficient remains below the specified value or the death rate of filter-feeding fish remains above the threshold, both populations can coexist.

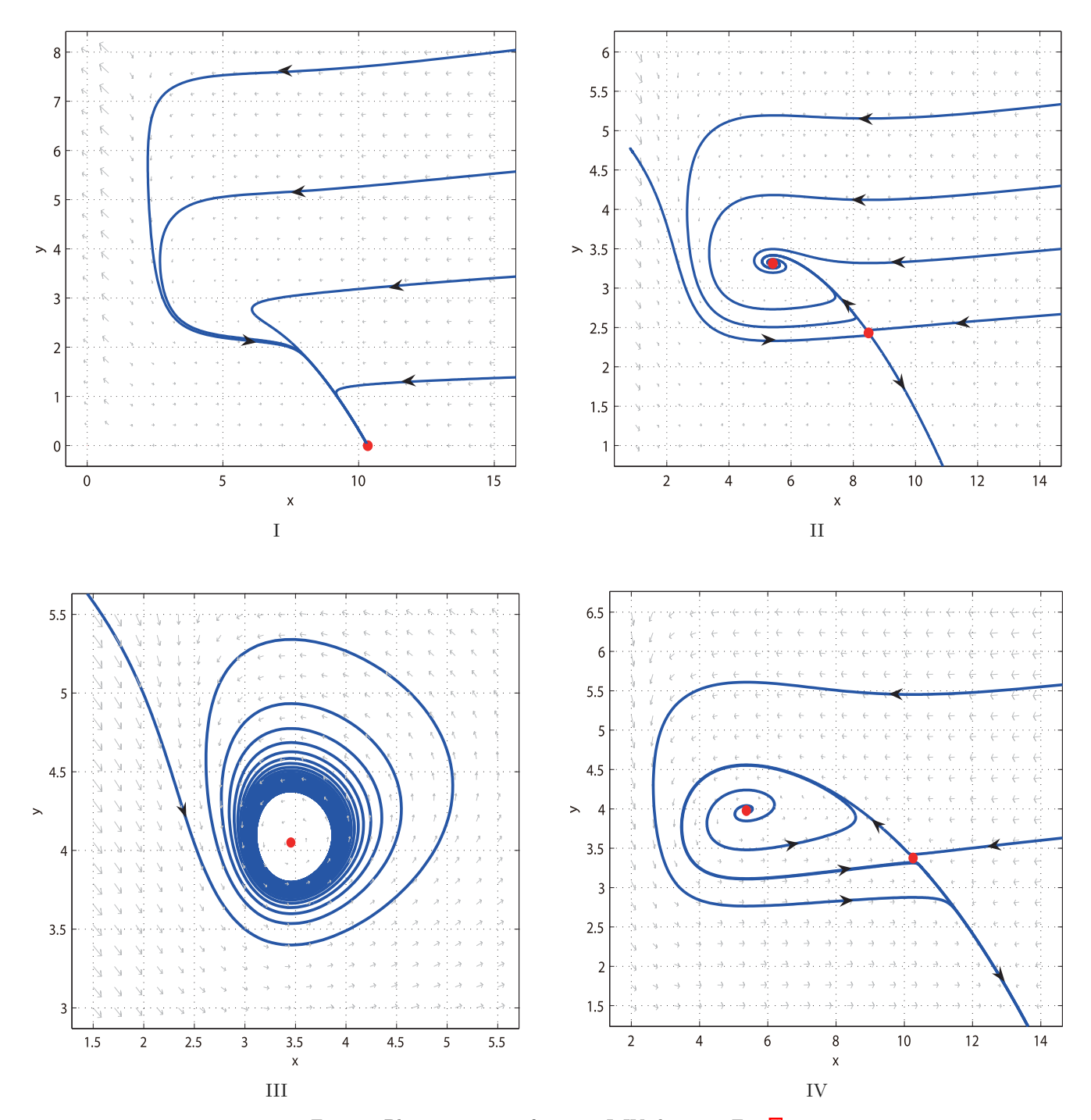


Fig. 5. Phase portraits of regions I–IV shown in Fig. \blacksquare

5. Conclusion and Discussion

This paper focuses on conducting a detailed bifurcation analysis of a new aquatic ecological model that incorporates Microcystis aeruginosa and filterfeeding fish, taking into account factors such as aggregation effect and harvesting. The analysis utilizes a dynamical system approach and investigates various types of bifurcations, including saddle-node bifurcation, Bogdanov–Takens bifurcation, and Hopf bifurcation.

The paper presents one-parameter bifurcation diagrams and two-parameter bifurcation diagrams involving the carrying capacity of Microcystis aeruginosa (k), harvesting (a), and the maximum harvesting rate of Microcystis aeruginosa (q). It is observed that the density of filter-feeding fish consistently increases with sustained oscillations as the density of Microcystis aeruginosa increases. However, if the maximum environmental capacity of Microcystis aeruginosa (k) is too small, it can lead to the extinction of filter-feeding fish.

Furthermore, the number of filter-feeding fish decreases progressively and eventually leads to extinction as the maximum harvesting rate of Microcystis aeruginosa (q) increases. To prevent the adverse consequences of blindly eliminating Microcystis aeruginosa, it becomes crucial to identify an optimal timing for harvesting Microcystis aeruginosa. This approach aims to enhance the yield of filter-feeding fish while maintaining ecological balance.

Acknowledgments

H. Zhang was supported by Key Research & Development project of the Science and Technology Department of Zhejiang Province (Grant No. 2021C02048), Y. Xu was partially supported by the National Natural Science Foundation of China (No. 11671114), L. Rong was supported by the National Science Foundation grant DMS-1950254.

References

- Auger, P., Kooi, B. W., Parra, R. B. D. L. & Poggiale, J. C. [2006] "Bifurcation analysis of a predator-prey model with predators using hawk and dove tactics," J. Theor. Biol. 238, 597-607.
- Chen, H. & Lurling, M. [2020] "Calcium promotes formation of large colonies of the cyanobacterium Microcystis by enhancing cell-adhesion," *Harmful Algae* 92, 101768.

- Cui, J. A. & Song, X. [2004] "Permanence of predator—prey system with stage structure," *Discr. Cont. Dyn. Syst. B* **4**, 547–554.
- Doedel, E. J., Champneys, A. R., Fairgrieve, T., Kuznetsov Yuri, Oldeman, B., Paffenroth, R., Sandstede, B., Wang, X. J. & Zhang, C. H. [2007] "Auto-07p: Continuation and bifurcation software for ordinary differential equations," https://www.macs.hw.ac.uk/gabriel/auto07/auto.html.
- Duan, Z., Tan, X., Parajuli, K., Zhang, D. & Wang, Y. [2019] "Characterization of microcystis morphotypes: Implications for colony formation and intraspecific variation," *Harmful Algae* 90, 101701.
- Duan, Y., Xiong, D., Wang, Y., Dong, H. & Zhang, J. [2020] "Effects of microcystis aerugnosa and microcystin-LR on intestinal histology, immune response, and microbial community in litopenaeus vannamei," Environ. Pollut. 265, 114774.
- Huang, S., Yu, H., Dai, C., Ma, Z., Wang, Q. & Zhao, M. [2022] "Dynamic analysis of a modified algae and fish model with aggregation and Allee effect," *Math. Biosci. Eng.* 19, 3673–3700.
- Huang, R., Guo, W., Liu, Z., Li, S., Zhao, Z., Shi, W., Cui, F. & Hu, C. [2023] "Variations in trihalomethane formation potential of microcystis aeruginosa under different growth conditions: Phenomenon and mechanism," Sci. Total. Environ. 892, 164440.
- Kolmakov, V. I. [2014] "Role of microcystis aeruginosa passing through the digestive tracts of filter-feeding animals in eutrophic water reservoirs," Contemp. Probl. Ecol. 7, 455–464.
- Li, X., Yu, H., Dai, C., Ma, Z. & Zhao, M. [2021] "Bifurcation analysis of a new aquatic ecological model with aggregation effect," *Math. Comput. Simul.* **190**, 75–96
- Lin, X., Xu, Y., Gao, D. & Fan, G. [2022] "Bifurcation and overexploitation in Rosenzweig-MacArthur model," Discr. Cont. Dyn. Syst. B 28, 690-706.
- Liu, J. & Zhang, L. [2016] "Bifurcation analysis in a prey-predator model with nonlinear predator harvesting," J. Franklin Inst. 353, 4701–4714.
- Liu, X. X. & Huang, Q. D. [2018] "The dynamics of a harvested predator–prey system with Holling type IV functional response," *Biosystems* **169**, 26–39.
- Liu, H., Yu, H., Dai, C., Ma, Z., Wang, Q. & Zhao, M. [2021] "Dynamical analysis of an aquatic amensalism model with non-selective harvesting and Allee effect," Math. Biosci. Eng. 18, 8857–8882.
- Lu, M., Xiang, C., Huang, J. & Wang, H. [2022] "Bifurcations in the diffusive Bazykin model," *J. Diff. Eqs.* **323**, 280–311.
- Lv, Y., Yuan, R. & Yu, P. [2013a] "A prey-predator model with harvesting for fishery resource with reserve area," Appl. Math. Model. 37, 3048-3062.
- Lv, Y., Yuan, R. & Yu, P. [2013b] "Two types of predator-prey models with harvesting: Non-smooth

- and non-continuous," J. Comput. Appl. Math. 250, 122–142.
- Lv, Y., Yu, P. & Wang, Y. [2019] "Bifurcations and simulations of two predator-prey models with nonlinear harvesting," *Chaos Solit. Fract.* **120**, 158–170.
- Pal, M., Yesankar, P. J., Dwivedi, A. & Qureshi, A.
 [2020] "Biotic control of harmful algal blooms (habs):
 A brief review," J. Environ. Manag. 268, 1–10.
- Perko, L. [1996] Differential Equations and Dynamical Systems (Springer, NY).
- Rihan, F. A., Alsakaji, H. J. & Rajivganthi, C. [2020] "Stability and Hopf bifurcation of three-species preypredator system with time delays and Allee effect," *Complexity* **2020**, 1–15.
- Sen, D., Morozov, A., Ghorai, S. & Banerjee, M. [2022] "Bifurcation analysis of the predator-prey model with the Allee effect in the predator," J. Math. Biol. 84, 1-27.
- Tang, H., Hou, X., Xue, X., Chen, R., Zhu, X., Huang, Y. & Chen, Y. [2017] "Microcystis aeruginosa strengthens the advantage of Daphnia similoides in competition with Moina micrura," Sci. Rep. 7, 10245.
- Thirthar, A. A., Majeed, S. J., Shah, K. & Abdeljawad, T. [2022] "The dynamics of an aquatic ecological model with aggregation, fear and harvesting effects," AIMS Math. 7, 18532–18552.
- Xie, P. & Liu, J. [2001] "Practical success of biomanipulation using filter-feeding fish to control cyanobacteria blooms: A synthesis of decades of research and application in a subtropical hypereutrophic lake," Sci. World J. 1, 337–356.

- Xu, Y. C., Zhu, Z. R., Yang, Y. & Meng, F. W. [2020] "Vectored immunoprophylaxis and cell-to-cell transmission in HIV dynamics," *Int. J. Bifurcation and Chaos* **30**, 1–19.
- Yang, Y., Meng, F. W. & Xu, Y. C. [2023] "Global bifurcation analysis in a predator-prey system with simplified Holling IV functional response and antipredator behavior," Math. Meth. Appl. Sci. 46, 6135-6153.
- Yu, H., Zhao, M. & Agarwal, R. P. [2014] "Stability and dynamics analysis of time delayed eutrophication ecological model based upon the Zeya reservoir," Appl. Math. Comput. 97, 53–67.
- Zhang, Y. S., Li, H. Y., Kong, F. X., Yu, Y. & Zhang, M. [2011] "Role of conony intercellular space in the cyanobacteria bloom-forming," Sci. World J. 32, 1602–1607.
- Zhang, J., Yu, M., Gao, Y., Zhang, M., Dong, J., Li, M. & Li, X. [2023] "Feeding behavior, microcystin accumulation, biochemical response, and ultramicrostructure changes in edible freshwater bivalve corbicula fluminea exposed to microcystis aeruginosa," Environ. Sci. Pollut. Res. 30, 13560–13570.
- Zhou, X. S., Li, H. F., Pan, M. M., Luo, Y. & Zhang, Z. G. [2013] "Study on phytoplankton community during the cyanobacteria bloom in Haihe River," Yellow River 35, 63–65.
- Zhu, Z. R., Wu, R. C., Yang, Y. & Xu, Y. C. [2023] "Modeling HIV dynamics with cell-to-cell transmission and CTL response," *Math. Meth. Appl. Sci.* 46, 6506–6528.